CORPUS PUBLISHERS

Journal of Mineral and Material Science (JMMS)

Volume 3 Issue 4, 2022

Article Information

Received date :September 20, 2022

Published date: October 10, 2022

*Corresponding author

Radiyah A Bahareth, University of Jeddah, College of Science, Department of Physics, Jeddah, Saudi Arabia

Keywords

Laser; Makrofol; Optical Properties; Color

Research Article

Radiation Induced Changes in Makrofol PCVM Polycarbonate

Radiyah A Bahareth*

University of Jeddah, College of Science, Department of Physics, Jeddah, Saudi Arabia

Abstract

Makrofol PCVM is a sort of Makrofol polycarbonate solid state nuclear track detector. It is worth mentioning that this paper is almost the first one that deals with the modification of the optical properties of this type of Makrofol under the effect of laser radiation. Samples from Makrofol PCVM were exposed to infrared pulsed laser with different fluences ranging from 15 to 125 J/cm^2. UV spectroscopic technique was used to obtain knowledge about the optical parameters that describe the samples under study. The changes of Urbach energy (E_u), optical band gap (E_g) and refractive index (n) with the laser fluence were investigated. Both E_u and n increased with increasing the fluence up to 125 J/cm^2, associated with a decrease of E_g values. These trends were assigned to the predominance of chain crosslinking that damaged the crystalline portion in the Makrofol polymer. Additionally, we used the CIE technique to calculate the color differences between the non-coloured pristine and the irradiated samples. The crosslinking created color centers that produced color difference between the exposed films and the uncolored pristine Makrofol film. The color difference was significant as the values of ΔE were greater than 5. This optimized the Makrofol polymer to be used in dosimetric applications.

Introduction

One of the most important characters in in materials processing is the laser. Laser sintering, for example, is usually applied in several applications [1]. Laser radiation is widely used to modify the characteristics of material's surface [2]. It produces structural properties in the surface that are essential of research [3,4]. Several changes in the polymeric matter properties, in the nano and microscales, take place due to the effect of laser radiation. The nonlinear ionization effect of laser causes the elimination of surface atoms in the treated area. This results in alternations of polymer properties [5]. Likewise, the changes in chemical properties of polymeric matter are almost appropriate processes for the production of nanomaterials, 3D photo-polymerization and laser lithography [6]. There are several sorts of Makrofol (bisphenol-A polycarbonate) Nuclear Track Detectors (NTDs). One of those is the used Makrofol PCVM that was manufactured for the use in the dosimetry. It is an amorphous polymer that possesses excellent properties that permitted it to be intense applicant in dosimetry [7-10]. The properties of Makrofol are dependent on the manufacture environments factors. Consequently, its characteristics change due to the radiations exposure [7]. The existence of carbonyl group represents one of the characteristic properties of Makofol as it degrades by the action of small doses of radiation [11]. Makrofol is appropriate for electronic devices and optical fibers due to its intense transparency and low density. These characteristics allowed it to be used in dosimetry. Also, we usually use Makrofol to get track etched films, neutron and alpha radiography, recognitions cosmic radiations, and in the gamma rays and ultraviolet radiation dosimetry [12-14]. Though Makrofol has enormous practical and saleable rank, some non-expected issues, such as humidity and temperature changes may be established during fabrication. This creates structural deficiencies in the Makrofol films, leading to variations in its chemical and physical characteristics. Radiation processing can reduce the induced structural defects.

The optical properties of irradiated polymers are extensively used in optoelectronic apparatuses [15]. Refractive indices of polymeric materials provide information concerning their vital properties [16]. Moreover, the changes in color owing to irradiation assess the optical characteristics of the matter. It is one of the most important methodologies that have been applied to assess physical changes in irradiated polymers. This is significant evidence for their application in commercial requests and dosimetry [17]. Some investigates were carried out to highlight the significance of color alternation of the irradiated polymers in the field of dosimetry [18-20]. They explored that the color change technique pledges the fundamentals which should be considered in the creation of radiation sensors. They attributed the change in color in irradiated polymers to the active free radicals increases the conjugated bonds [21]. Additionally, they attributed the variation of color in exposed Makrofol to radical species, relieved benzophenones, and extremely conjugated bonding or rearranged isopropylidene radicals. The present study aims to modify the optical properties of Makrofol PCVM to be suitable for numerous applications. Moreover, the study of color changes introduces the basis that can be used in constructing simple sensor for irradiation.

Experimental

Materials

Makrofol PCVM sheets are clear translucent polycarbonates manufactured by Farbenfabriken Bayer A.G., Germany. The sheets were 250 μm thick and had a density of 1.2 g/cm^3. They had a light transmission of 90%. The chemical formula is $C_{16}H_{14}O_3$.

Irradiation tool

We used 5 watt pulsated GaAs laser of 904 nm wavelength. The frequency and pulse duration were 1200 Hz and 200 ns, correspondingly. The diameter of the circular shaped pulse, of a Gaussian profile, was 6 mm and the spot area was 0.28 cm^2.

Methodology

A Tomos spectrophotometer, Model No. 1800 was used to record the UV absorbance spectra. The Commission International de E'Claire (CIE) methodology was used to estimate the changes in color in the samples under study. Detailed information concerned the color alternation calculations were given in a previous work [15]. The CIE method is dependent on the explanation of color as luminance components X, Y and Z. Their spectral weighting curves have been standardized

by the CIE based on statistics from trials concerning human viewers. The amounts of the X, Y and Z constituents are proportional to physical energy, but their spectral configuration corresponds to the color matching appearances of human vision. The vision scientists formed a special set of mathematical lights, X, Y and Z, to replace the actual red, green and blue lights known as the color's tristimulus values [22]. The 1976 CIE intercepts a*, b* and b* denote the green–red, blue–yellow and dark–white axes, respectively. The accuracy in calculating L* is ±0.05 and is ±0.01 for both a* and b*, correspondingly.

The color intensity (color difference), ΔE is:

$$\Delta E = \left[(L_1^* - L_2^*)^2 + (a_1^* - a_2^*)^2 + (b_1^* - b_2^*)^2 \right]^{1/2} \quad (1)$$

The subscripts 1 and 2 mention to the exposed and pristine samples.

Results and Discussion

Analysis of the absorption

We performed the absorbance study to get information concerning the optical micro-electronic transitions. This explains the optical bandgap (E_g) and studies its dependence on the laser fluence. Figure 1 shows the variation of the absorbance with the wavelength for the non-exposed and exposed Makrofol samples. We attribute the decrease of absorbance with increasing the wavelength to the reduced number of phenyl group (π– π*) transitions and (n– π*) carbonyl group [16]. Moreover, the absorbance of the Makrofol films increased with increasing the fluence up to 125 J/cm^2. This can be due to the increase of bonding via crosslinking. The energy transferred by the incident laser photons creates new chemical arrangement enhancing the absorbance [17].

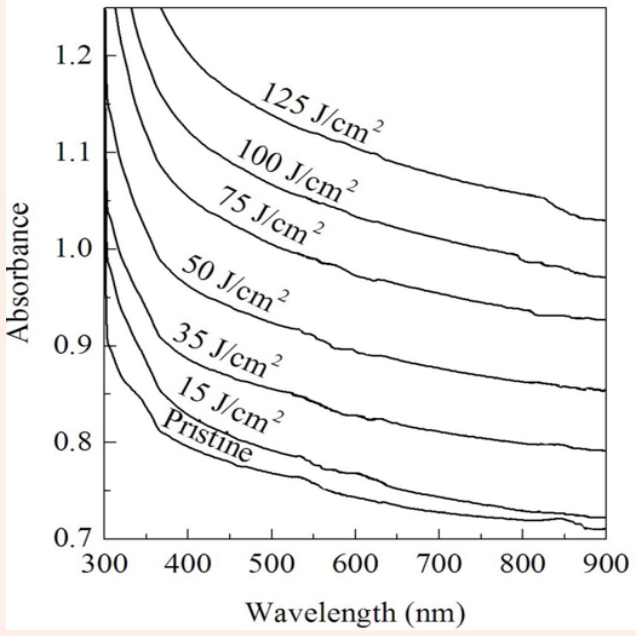

Figure 1: The UV-Vis absorbance spectra of the Makrofol films.

Analysis of urbach energy

An essential factor that provides knowledge concerning the fractional dispersal of the incident radiation when scattered and absorbed by the penetrated medium is the extinction coefficient (k). We calculated the values of k by means of : 4

$$k = \left(\lambda \alpha / 4\pi \right) \quad (2)$$

Where, λ is the wavelength and α means the absorption coefficient that can be computed from:

$$\alpha = Absorbance \times 2.303 / thickness\ of\ the\ sample \quad (3)$$

It is seen in Figure 1 that there is an exponential rise in the absorbance near to the edge that matches the movement from the localized states in the valence band tail. In amorphous polymers there are tail states seem in the gap area below the main absorption edge [18]; that can be estimated using the absorption coefficient (α) in the Urbach rule [19];

$$\alpha = \alpha_o \exp\left(\frac{h\upsilon}{E_U} \right) \quad (4)$$

Where, α_o is constant determines the matter and E_u is the Urbach energy that means the tail width of localized states in the forbidden bandgap [20] and hn is the energy of the photon. We calculated the values of E_u from the slope of exponential dependence of absorption coefficient edge vs. hn. The variation of E_u with the laser fluence is shown in Figure 2. The values of E_u increased with increasing the fluence up to 125 J/cm^2. This can be attributed to the increase of the amorphous phase due to the action of laser radiation [21,22].

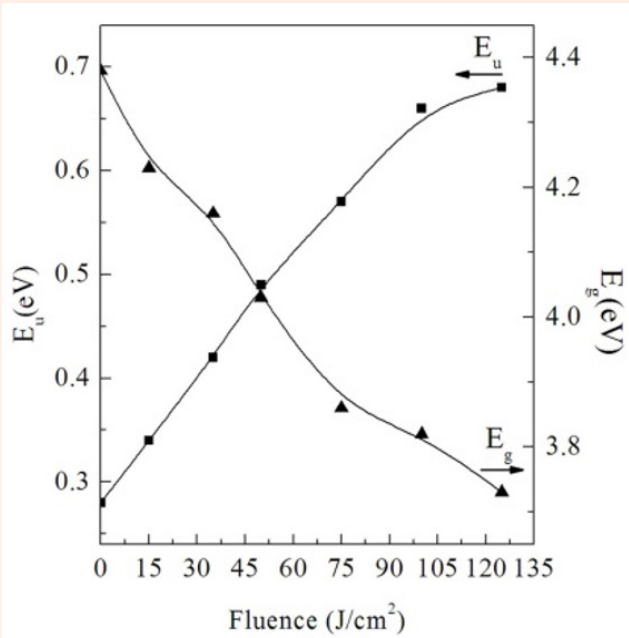

Figure 2: The change of E_u and E_g with the laser fluence.

Analysis of bandgap

The bandgap (E_g) was calculated applying Tauc's principle [23]:

$$\alpha h\upsilon = B\left(h\upsilon - E_g \right)^n \quad (5)$$

Where, B is a constant, hν is the photon energy and the n is an index of explores the trend of the micro-electronic transition. If the value of n is 1/2 or 3/2 then the transition is direct, whereas if n is 2 or 3, the transition is allowed or forbidden indirect [24]. The E_g numerical values were calculated by drawing (αhn)1/n against hn and extending the linear segment of the plot at the hn axis (Figure 3).

The dependence of E_g on the laser fluence is displayed in Figure 2. The E_g values decreased with increasing the fluence up to 125 J/cm^2. The decrease in E_g can be assigned to crosslinking that enhances the amorphous phase of the Makrofol sheets. This produces deficiencies in the structure, permitting the creation of localized states in the E_g structure originating lesser energy micro-electronic transitions. Then, the substantial action of the laser radiation on the films was the formation of free radicals which produced the growth of the conjugated bonds and hence decreasing the E_g.

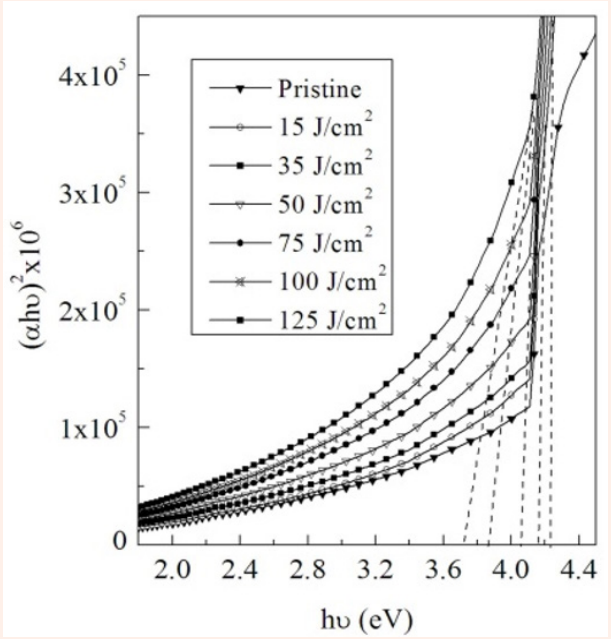

Figure 3: A Plot of (αhν)2 versus hν.

Analysis of the refractive index

The refractive index, n, of the Makrofol films is calculated using the formula [25]:

$$\left(\frac{n^2-1}{n^2+1}\right)=1-\sqrt{\frac{E_g}{20}} \quad (6)$$

The variation of n with the laser fluence is shown in Figure 4. The values of n increased with increasing fluence up to 125 J/cm². The obtained behavior agrees with that of E_g, both due to the occurrence of crosslinking. The chain scissions create active free radicals that result in the creation of covalent bonds via crosslinks. This investigation agrees well with that obtained previously [26].

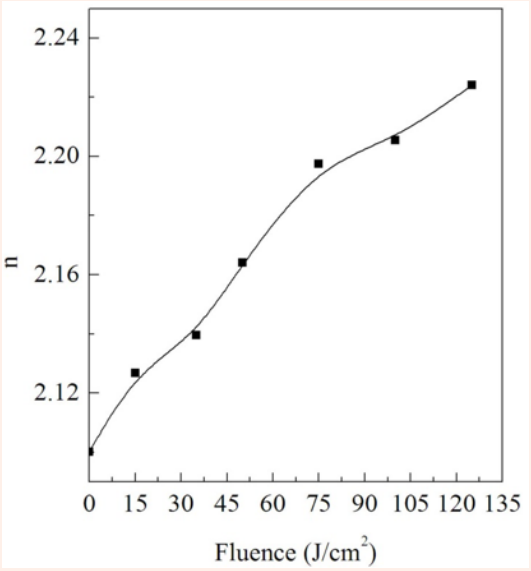

Figure 4: The change of refractive index with the laser fluence.

Color difference measurements

The calculation of color differences with change in the radiation fluences is an important issue of nuclear track detectors. The color parameters were calculated by means of the transmission values (370-780 nm). The tristimulus values were estimated and represented in Figure 5 versus laser fluence. Their values reduced on raising the laser fluence up to 125 J/cm². Additionally, the chromaticity coordinates were calculated and displayed in Figure 6 versus laser fluence. The x and y coordinates increased with increasing the fluence to 125 J/cm², whereas, the z coordinate decreased. The variations of color intercepts a* and b* with the laser fluence are presented in Figure 7. The a* and b* intercepts displayed negative values that increased with increasing the fluence up to 125 J/cm², investigating the change of the green color component into red and the blue to yellow, respectively. This was correlated to the development of darkness in the Makrofol (–L*) (Figure 8).

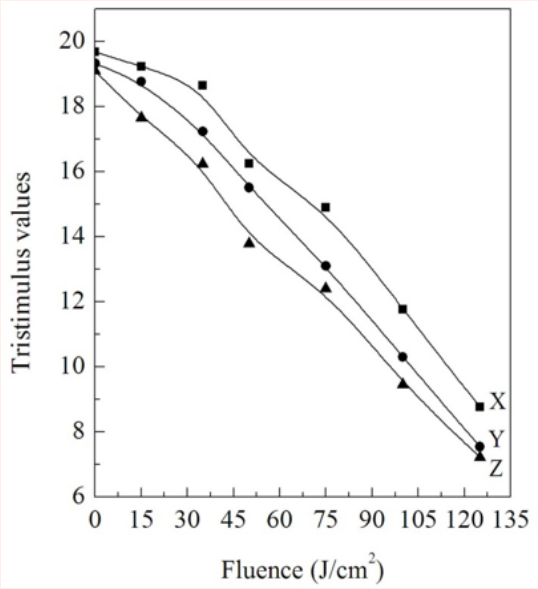

Figure 5: The change of tristimulus values with the laser fluence.

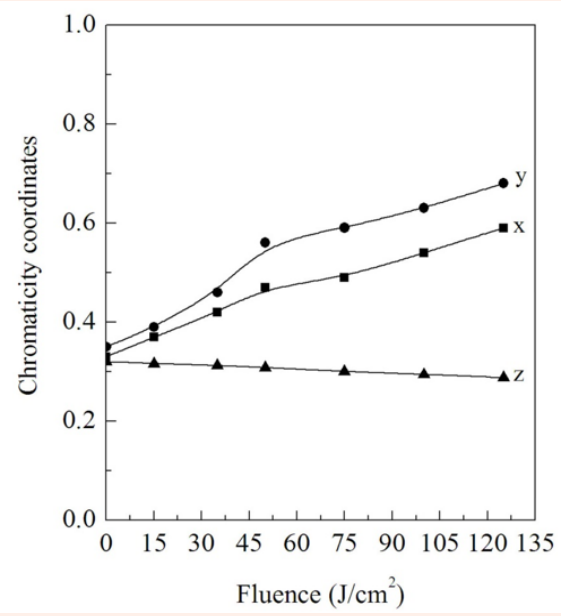

Figure 6: The change of chromaticity coordinates with the laser fluence.

The color intensity (ΔE) was calculated using equation 1 and is plotted in Figure 8 against laser fluence. An increase of ΔE was observed on increasing the fluence up to 125 J/cm^2. The values of ΔE were more than 5. This indicates a significant color change [27,28]. The change in color of Makrofol due to laser exposure can be due to the free radicals, re-arranged isopropylidene radicals, formation of strong conjugated bonds and the benzophenones [21]. The resultant free radicals are chemically active and thus take part in chemical reactions causes crosslinking. This was associated with the creation of color centers. Additionally, these active free radicals that have electrons with unpaired spin, cause color variations [15].

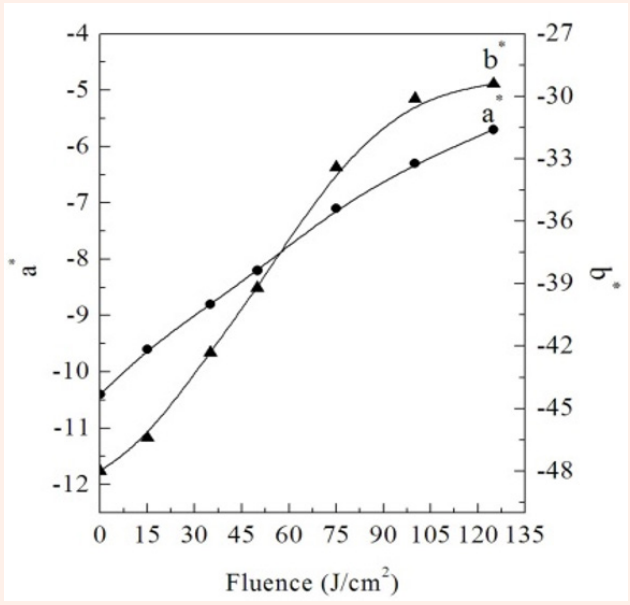

Figure 7: The change of a* and b* intercepts with the laser fluence.

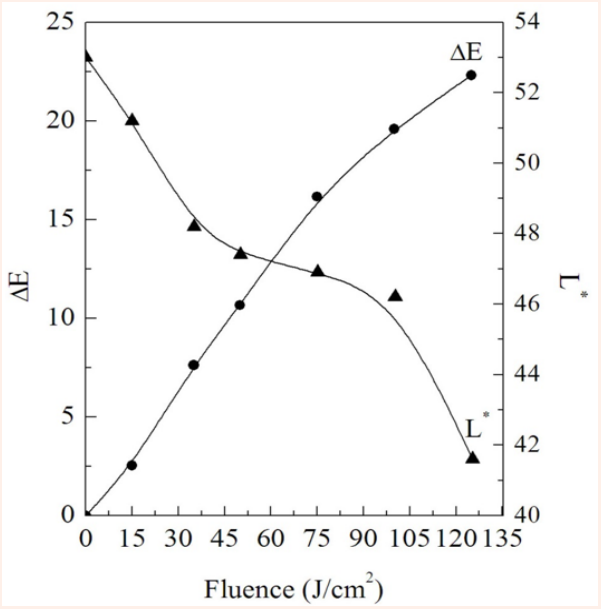

Figure 8: The change of L* and color intensity DE with the laser fluence.

Conclusion

The laser irradiation with fluences up to 125 J/cm^2 causes the prevalence of crosslinking that altered the optical character of Makrofol and permitted it to be used optoelectronic tools. Moreover, the Makrofol displayed significant color variation due to laser exposure, which is an important property for the used in dosimetry.

References

1. Sivadas BO, Ashcroft I, Khlobystov AN, Goodridge RD (2021) Laser sintering of polymer nanocomposites. Advanced Industrial and Engineering Polymer Research 4(4): 277-300.
2. Li M, Lu QH, Yin J, Qian Y, Wang ZG (2002) Effects of post-thermal treatment on preparation of surface microstructures induced by polarized laser on polyimide film. Mater Chem Phys 77(3): 895-898.
3. Pelletier H, Nelea V, Mille P, Muller D (2004) Mechanical properties of pulsed laser-deposited hydroxyapatite thin film implanted at high energy with N+ and Ar+ ions. Part I: Nanoindentation with spherical tipped indenter. Nucl Inst Meth B 216(1): 269-274.
4. Christian R, Christropher G, Roland H, Jens L, Pierre B, et al. (2004) First laser ions at an off-line mass separator of the ISAC facility at TRIUMF. Nucl Inst Meth B 215(1-2): 268-277.
5. Awasthi S, Little DJ, Fuerbach A, Kane DM (2021) Polymer like response of muscovite upon 515 nm femtosecond laser pulse processing. Optics and Laser Technology 135: 106641.
6. Rebollar E, Castillejo M (2020) Laser interactions with organic/polymer materials. In: Sugioka K (Ed.), Handbook of Laser Micro- and Nano-Engineering, Springer International Publishing, pp. 1-49.
7. El Ghazaly M, Aydarous A (2017) Photoluminescence emission spectra of Makrofol® DE 1-1 upon irradiation with ultraviolet radiation. Results Phys 7: 333-337.
8. Yu KN, Nikezic D (2009) Nuclear track detectors: design, methods and applications. Nova Science Publishers, New York, USA, pp. 107-131.
9. Singh NL, Qureshi A, Singh F, Avasthi DK (2007) Modifications of polycarbonate induced by swift heavy ions. Mater Sci Eng A 457(1-2): 195-198.
10. Durrani SA, Bull RK (1987) Solid state nuclear track detection: Pergamon Press, Oxoford, UK.
11. Nouh SA, Amer H, Remon SW (2009) Effect of neutron dose on the structural properties of Makrofol polycarbonate. Nucl Instrum Methods Phys Res B 267(7): 1129-1134.
12. Al-Amri A, El Ghazaly M, Abdel-Aal MS (2017) On induced-modifications in optical properties of Makrofol® DE 1-1 SSNTD by UVB and UVA. Results in Physics 7: 1361-1366.
13. Bahareth RA, Barakat MME, Alhodaib A, Aldawood S, Nouh SA (2021) Tailoring the optical properties of PC/ZnS nanocomposite by gamma radiation. Eur Phys J Appl Phys 93: 50402.
14. Al Naim A, Alnaim N, Ibrahim SS, Metwally SM (2017) Effect of gamma irradiation on the mechanical properties of PVC/ZnO polymer nanocomposite. J Radiat Res Appl Sci 10(3): 165-171.
15. Nouh SA, Gaballah N, Abou Elfadl A, Alsharif SA (2019) Modification induced by proton irradiation in bayfol UV1 7-2 nuclear track detector. Radiat Protect Dosimet 183(4): 450-459.
16. Nouh SA, Atta MR, El-Melleegy WM (2004) A Study of the effect of gamma and laser irradiation on the thermal, optical and structural tract detector. Radiat Eff Defect Solid 159(8-9): 461-474.
17. Nouh SA, Radwan Y, Elfiky D, Abutalib M, Bahareth R, et al. (2014) Structure, thermal, optical and electrical investigation of the effect of heavy highly energetic ions irradiations in Bayfol DPF 5023 nuclear track detector. Radiat Phys Chem 97: 68-74.
18. Rakhshani AE (2000) Study of Urbach tail, bandgap energy and grain-boundary characteristics in CdS by modulated photocurrent spectroscopy. J Phys: Condens Matter 12(19): 4391.

19. Urbach F (1953) The long-wavelength edge of photographic sensitivity and of the electronic absorption of solids. Phys Rev 92(5): 1324.

20. Wahab LA, Zayed HA, Abd El-Galil AA (2012) Study of structural and optical properties of Cd1-xZnxSe thin films. Thin Solid Films 520(6): 5195-5199.

21. Prasher S, Kumar M, Singh S (2014) Electrical and optical properties of O6+ ion beam–irradiated polymers. Int J Polym Anal Charact 19(3): 204-211.

22. Sharma R, Kamal KK, Das MK, Gupta GK, Kumar S (2016) Short carbon fiber-reinforced polycarbonate composites. In: Kar KK (Ed.), Composite Materials Processing, Applications, Characterization: Springer, Berlin, pp. 199-223.

23. Tauc J (1972) Optical properties of solids. In: Abeles F (Ed.), Elsevier, Amsterdam, North-Holland, Netherlands, p. 77.

24. Aziz SB, Abdullah OG, Hussein AM, Ahmed HM (2017) From insulating PMMA polymer to conjugated double bond behavior: green chemistry as a novel approach to fabricate small band gap polymers. Polymers 9(11): 626.

25. Elkhoshkhany N, Abbas R, El-Mallawany R, Fraih A (2014) Optical properties of quaternary TeO_2–ZnO–Nb_2O_5–Gd2O3 glasses. J Ceram Int 40(9): 14477-14481.

26. Shams-Eldin MA, Wochnowski C, Koerdt M, Metev S, Hamza AA, et al. (2005) Characterization of the optical-functional properties of a waveguide written by an UV-laser into a planar polymer chip. Opt Mater 27(6): 1138-1148.

27. Benthami K, Barakat MME, Nouh SA (2020) Modification of optical properties of PC-PBT/Cr_2O_3 and PC-PBT/CdS nanocomposites by gamma irradiation. Eur Phys J Appl Phys 92(2): 20402.

28. Nouh SA, Barakat MME, El-Nabrawy HA, Benthami K, Elhalawany N (2021) Color changes in some UV irradiated polymer nanocomposite materials for the application in textile industry. Fibers Polym 22: 1711-1717.